



# The Effectiveness of CT Metal Artifact Reduction Technique and Its Contribution to Radiological Evaluation in Lumbar Stabilization

## Lomber Stabilizasyonda BT Metal Artefakt Azaltma Tekniğinin Etkinliği ve Radyolojik Değerlendirmeye Katkısı

✉ Nuri Serdar Baş<sup>1</sup>, ✉ Serap Baş<sup>2</sup>

<sup>1</sup>University of Health Sciences Turkey, İstanbul Bağcılar Training and Research Hospital, Clinic of Neurosurgery, İstanbul, Turkey

<sup>2</sup>İstanbul Yeni Yüzyıl University Faculty of Medicine, Department of Radiology, İstanbul, Turkey

### Abstract

**Objective:** Metal artifact reduction (MAR) systems, which have been patented by the firms and specific to them, have been developed to reduce the losses in the images, which are caused by artifacts, and to increase the diagnostic value of computed tomography (CT). The objective of this study is to determine the effectiveness of the MAR technique, which minimizes the image loss caused by metal artifacts in CTs taken for the lumbar spinal region where metallic implants are located, and its contributions to radiological evaluation.

**Method:** Patients with spinal stabilization, whose CT imaging records of both standard and smartMAR (SMAR) reconstruction were performed between June 2020 and March 2021 and could be accessed, were evaluated. Critical anatomical structures were defined as: spinal canal (SC), neural foramen (NF), and prevertebral-paravertebral area (P-PA). The image quality of critical anatomical structures were evaluated using a 5-point image quality scale for soft tissue (400/35 HU) and bone window settings (2,500/480 HU) on standard and SMAR reconstructed CT images. In addition, the size of the flame artifact was measured and recorded in millimeters in standard and SMAR images.

**Results:** Of the 24 patients with lumbar spinal stabilization who met the inclusion criteria, 8 were male, and 16 were female (66%). The age range was determined to be between 26 and 82 years (mean=60). The stabilization of all patients was in the form of posterior transpedicular screw and rod fixation. The radiation dose distribution ranged between 3.23 and 14.1 millisieverts (mSv) (mean=8.95 mSv). The worst visualization score was obtained on SC imaging, which was evaluated in the soft tissue window. In bone window evaluations of these structures, the visualization

### Öz

**Amaç:** Radyolojik görüntülerde artefakta bağlı oluşan kayıpları azaltmak ve çekilen bilgisayarlı tomografinin (BT) tanısal değerini artırmak üzere firmalara özel patentli metal artefaktı azaltma (MAR) sistemleri geliştirilmiştir. Bu çalışmanın amacı, metalik implantların bulunduğu lomber spinal bölgeye yönelik çekilen BT'lerde, metal artefaktından kaynaklanan görüntü kayıplarını minimize etmeye yarayan MAR tekniğinin etkinliğini ve radyolojik değerlendirmeye katkılarını belirlemektir.

**Yöntem:** Haziran 2020-Mart 2021 tarihleri arasındaki dönemde, spinal stabilizasyonu olan hem standart hem de smartMAR (SMAR) rekonstrüksiyon uygulanmış BT kayıtlarına ulaşılan hastalar değerlendirildi. Kritik anatomik yapılar olarak tanımlanan spinal kanal (SK), nöral foramenler (NF) ve prevertebral-paravertebral alan (P-PA), standart ve SMAR rekonstrüksiyonlu BT görüntülerinde, yumuşak doku (400/35 HU) ve kemik pencere (2,500/480 HU) için 5 puanlı görüntü kalite ölçeği kullanılarak değerlendirildi. Ayrıca, alev artefaktının boyu standart ve SMAR'li görüntülerde milimetre olarak ölçülerek kaydedildi.

**Bulgular:** Çalışmaya dahil edilme kriterlerini karşılayan lomber spinal stabilizasyonlu 24 hastanın, 8'i erkek ve 16'sı kadını (%66). Yaş aralığı 26-82 yaş arasında (ortalama=60) bulundu. Hastaların hepsinin stabilizasyonu posterior transpediküler vida ve rod fiksasyon şeklindeydi. Radyasyon doz dağılımı 3,23 ile 14,1 milliSievert (mSv) (ortalama=8,95 mSv) arasındaydı. En kötü vizualizasyon skoru yumuşak doku penceresinde değerlendirilen SK görüntülemesinde elde edildi. Bu yapıların kemik pencere değerlendirmelerinde, SK için vizualizasyon skorları (medyan) standart ve SMAR'li görüntülemelerde sırasıyla 3 ve 4 (Z=-3,926, p<0,001), NF için 4 ve 5 (Z=-3,666, p<0,001), P-PA için 4



**Address for Correspondence:** Nuri Serdar Baş, University of Health Sciences Turkey, İstanbul Bağcılar Training and Research Hospital, Clinic of Neurosurgery, İstanbul, Turkey

**E-mail:** nserdarbas@yahoo.com.tr **ORCID:** orcid.org/0000-0003-1625-4868 **Received:** 08.04.2021 **Accepted:** 08.07.2021

**Cite this article as:** Baş NS, Baş S. The Effectiveness of CT Metal Artifact Reduction Technique and Its Contribution to Radiological Evaluation in Lumbar Stabilization. Bagcilar Med Bull 2021;6(3):264-270

©Copyright 2021 by the Health Sciences University Turkey, Bağcılar Training and Research Hospital  
Bagcilar Medical Bulletin published by Galenos Publishing House.

## Abstract

scores (median) in standard and SMAR imaging's were found to be 3 and 4 ( $Z=-3.926$ ,  $p<0.001$ ) for SC, 4 and 5 for NF ( $Z=-3.666$ ,  $p<0.001$ ), and 4 and 5 ( $Z=-4.203$ ,  $p<0.0001$ ) for P-PA, respectively. These differences were also significant. Bone cortex visualization score (median), measured on bone window images, were determined to be 4 (minimum:2, maximum:5) and 5 (minimum:4, maximum:5) ( $Z=-4.028$ ,  $p<0.0001$ ) in standard and SMAR imagings, respectively. As an objective criterion, the flame artifact length, which was evaluated only in bone window images, was 26 mm on average (standard deviation  $\pm 9.78$ ) (minimum:8, maximum:54 mm) in standard imaging, whereas it decreased to 3.66 mm (standard deviation  $\pm 2.54$ ) (minimum:0, maximum:7 mm) in reconstructions via SMAR.

**Conclusion:** The MAR technique significantly reduces the artifacts occurring with standard techniques in adjacent tissues applied for medical treatment purposes and allows a clearer evaluation of this region by the radiologist. The use of this technique enhances the quality of CT images and the diagnostic value of radiological examination. However, there is a need for the development of MAR software for optimal imaging.

**Keywords:** Computed tomography, flame artifact, lumbar stabilization, metal artifact

## Öz

ve 5 ( $Z=-4.203$ ,  $p<0.0001$ ) olarak bulundu. Bu farklar da istatistiki olarak anlamlıydı. Kemik pencere görüntülerinde ölçüm yapılan kemik korteks vizualizasyon skoru (medyan), standart ve SMAR'li çekimlerde sırasıyla 4 (minimum:2, maksimum:5) ve 5 (minimum:4, maksimum:5) ( $Z=-4.028$ ,  $p<0.0001$ ) olarak bulundu. Objektif kriter olarak değerlendirilen alev artefakt boyu standart çekimlerde ortalama 26 mm (standart sapma  $\pm 9.78$ ) (minimum:8, maksimum:54 mm) iken SMAR'li rekonstrüksiyonlarda 3,66 mm'ye (standart sapma  $\pm 2,54$ ) (minimum:0, maksimum:7 mm) düştü.

**Sonuç:** MAR tekniği, komşu dokularda oluşan artefaktları belirgin olarak azaltmakta ve radyolog tarafından bu bölgenin daha net değerlendirilebilmesine imkan vermektedir. Bu tekniğin kullanımı, BT görüntülerinin kalitesini ve radyolojik incelemenin tanılabilirliğini artırır. Ancak optimal görüntüleme için MAR yazılımlarının geliştirilmesine ihtiyaç vardır.

**Anahtar kelimeler:** Alev artefakt, bilgisayarlı tomografi, lomber stabilizasyon, metal artefakt

## Introduction

The use of spinal metallic instrumentation for medical applications such as instability and/or reducing pain is considerably common in neurosurgery practice. The number and variety of these stabilization surgeries have increased gradually over the years (1). Computed tomography (CT) and magnetic resonance imaging (MRI) are used for both the diagnosis and postoperative follow-up evaluation of the patients. Hence, metallic artifacts are often encountered in spinal imaging (2). The lumbar region is the spinal area where metallic stabilization material is used mostly. Artifacts related to spinal stabilization materials in standard CT and MRI scans reduce diagnostic confidence by hiding the anatomy and/or pathology in adjacent tissues (2-4). Because of this, metal artifact reduction (MAR) systems, which have been patented by the firms and are specific to them, have been developed for modalities both to reduce the losses in the images, which are caused by artifacts, and to increase the diagnostic value of CT and MRI (2). The objective of this study is to determine the effectiveness of the MAR technique, which minimizes the image loss caused by metal artifacts in CTs taken for the lumbar spinal region where metallic implants are located, and its contributions to radiological evaluation.

## Materials and Methods

This study was performed in line with the principles of the Declaration of Helsinki. Approval was granted by the

Ethics Committee of İstanbul Yeni Yüzyıl University (date: 05.04.2021/no. 2021/04-653). Informed consent forms were obtained from the patients before the CT procedure.

Patients with spinal stabilization, whose CT imaging records of both standard and SMAR reconstruction were performed between June 2020 and March 2021 and could be accessed, were evaluated. Patients who had only CT imaging with standard technique and did not have MAR reconstruction, as well as the patients who underwent CT scans for regions other than the lumbar region, were excluded from the evaluation. Twenty-four lumbar stabilization patients who met these criteria were included in the study.

## CT Acquisition and Image Reconstruction

The CT examinations were performed with a single source, 512 slice multidetector CT scanner (Revolution CT, GE Healthcare, Milwaukee, WI). The scanning mode had the following parameters: Tube voltage 120 kVp assist mode, tube current SmartmA mode (100-500 mA), detector coverage 40 mm, helical pitch 0.0992, rotation time 0.80 s, slice thickness 1.25 mm, slice interval 1.25 mm, and scan FOV 50 cm.

CT images were reconstructed by using a conventional (standard) weighted filtered back-projection (wFBP) and prototype SMAR algorithm (spine parameters). SMAR was performed by using a vendor-specified "spine" setting, which entails predetermined SMAR reconstruction parameters appropriate for spinal anatomy and hardware.

Each study was evaluated by viewing wFBP and SMAR images side-by-side, first with soft tissue settings [window width, 400 hounsfield units (HU); window level, 35 HU] and subsequently with bone window settings (window width, 2500 HU; window level 480 HU). Images were only evaluated in the axial plane without multiplanar reformations. After reconstructions, images were loaded onto the Advantage Windows Workstation 4.7 (GE Healthcare, Milwaukee, Wisconsin/USA) for viewing.

### Subjective Evaluation Criteria and Image Analysis

As the study was limited to the instrumentations in the lumbar region, critical anatomical structures were defined as: spinal canal (SC), neural foramen (NF), and prevertebral-paravertebral area (P-PA). Two radiologists concurrently evaluated the image quality of critical anatomical structures using a 5-point image quality scale for soft tissue (400/35 HU) and bone window settings (2.500/480 HU) on standard and SMAR reconstructed CT images of the same patient, which was placed side by side (Figure 1, 2). The scale was rated as follows: 1) Severe artifact with invisibility of surrounding structures. 2) Obvious artifacts with significant distortion and insufficient identification of surrounding structures. 3) Moderate artifacts that allow identification of surrounding structures. 4) Mild artifacts with blurring of surrounding structures. 5) No artifacts. A total of 12 separate scorings was made by assessing the soft tissue and bone window separately for the standard and SMAR images of critical anatomical structures.

Moreover, the bone cortex visualization score was evaluated in standard and SMAR imagings, only in bone window images, and scored based on the same scale. The joint scoring decisions of the radiologists were recorded as the visualization score. This procedure was applied to all patients.

Scoring values of 3 and above were diagnostically significant.

### Objective Evaluation Criteria

For an objective evaluation, the “flame” artifact, which reflects the length of intense beam hardening and is seen as a dark zone at the tip of the metal, was measured parallel to the pedicle screw in the vertebra. For this measurement, the linear dark band emerging from the screw tip was measured and recorded in millimeters on both standard and SMAR images (Figure 3).

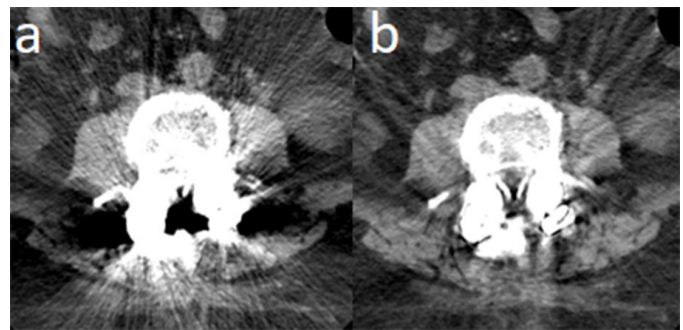


**Figure 1.** The spinal canal is obscured by artifacts on standard (a) image with soft-tissue window settings. SMAR (b) image with soft-tissue window settings at the same level improved visualization of the spinal canal

SMAR: Smart metal artifact reduction

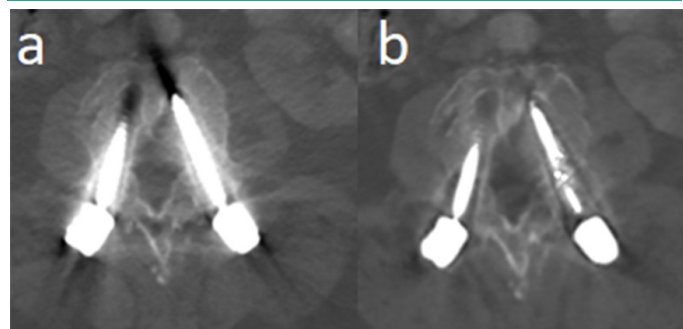


**Figure 2.** A 72-year-old woman status post L3- to-L5 pedicle screw. Standard (a) and SMAR (b) images at the L5 level using bone window settings demonstrate lucency about both L5 screws, consistent with hardware loosening

SMAR: Smart metal artifact reduction

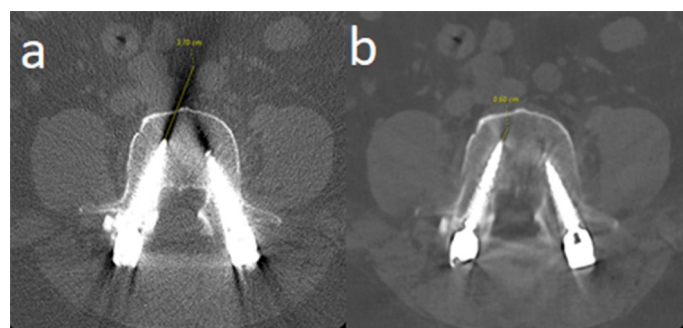


**Figure 3.** Extent of the flame artifact was measured in millimeters from the tip of the metal object to the end of the linear dark band at the same level on both standard (a) and SMAR images (b). Improvement in artifact severity is demonstrated on the SMAR image

SMAR: Smart metal artifact reduction

### Statistical Analysis

The Wilcoxon signed-rank test was performed by comparing the categorical scores provided by the radiologists for critical anatomical structures (lumbar SC, NF, pre-paravertebral

**Table 1. Standard and SMAR, subjective and objective analysis results**

Radiologist evaluation	Standard (min-max)			SMAR (min-max)			p
	SC	NF	P-PA	SC	NF	P-PA	
<b>Subjective (median)</b>							
-Soft-tissue window visualization score	1 (1-2)	3 (1-4)	2 (1-4)	3 (2-3)	4 (3-5)	4 (3-5)	p<0.0001
-Bone window visualization score	3 (1-5)	4 (2-5)	4 (1-5)	4 (3-5)	5 (3-5)	5 (4-5)	p<0.0001
-Bone cortex visualization score	4 (2-5)			5 (4-5)			p<0.0001
<b>Objective (mean)</b>							
-Length of flame artifact (mm)	26 (8-54)			3.66 (0-7)			p<0.0001

SC: Spinal canal, NF: Neural foramen, P-PA: Prevertebral-paravertebral area, SMAR: Smart metal artifact reduction

area) using standard and SMAR in soft tissue and bone window images, depending on the image quality and the ability to evaluate. The paired t-test was used to compare flame artifacts on standard and SMAR images, as the data were normally distributed (SPSS 13.0, SPSS Inc., Chicago, IL). For all comparisons, statistical significance was defined as  $p < 0.05$ .

## Results

Of the 24 patients with lumbar spinal stabilization, who met the inclusion criteria, 8 were male and 16 were female (66%). The age range was determined to be between 26 and 82 years (mean=60). The stabilization of all patients was in the form of posterior transpedicular screw and rod fixation. The number of stabilization segments was determined to be at least 2 and at most 9 (from dorsal to sacral) (median=3). The radiation dose distribution ranged between 3.23 and 14.1 millisievert (mSv) (mean=8.95 mSv).

### Evaluation of Critical Anatomical Structures

Scores of critical structures from subjective criteria evaluated in the lumbar region (soft tissue and bone window, median, minimum-maximum), bone cortex visualization scores (only in bone window), and flame artifact length (only in bone window and mean value) as objective criteria scores and statistical data about these values are presented in Table 1.

In the evaluation of critical anatomical structures in the soft tissue window, the visualization scores (median) in standard and SMAR imagings were determined to be 1 and 3 ( $Z = -4.16$ ,  $p < 0.0001$ ) for SC, 3 and 4 ( $Z = -4.420$ ,  $p < 0.0001$ ) for NF, and 2 and 4 ( $Z = -4.367$ ,  $p < 0.0001$ ) for P-PA, respectively, and the differences between them were statistically significant. The worst visualization score was obtained on SC imaging,

which was evaluated in the soft tissue window. In bone window evaluations of these structures, the visualization scores (median) in standard and SMAR imagings were found to be 3 and 4 ( $Z = -3.926$ ,  $p < 0.001$ ) for SC, 4 and 5 for NF ( $Z = -3.666$ ,  $p < 0.001$ ), and 4 and 5 ( $Z = -4.203$ ,  $p < 0.0001$ ) for P-PA, respectively. These differences were also significant.

Bone cortex visualization scores (median) measured on bone window images were determined to be 4 (minimum:2, maximum:5) and 5 (minimum:4, maximum:5) ( $Z = -4.028$ ,  $p < 0.0001$ ) in standard and SMAR imagings, respectively.

### Objective Artifact Evaluation Measurements

As an objective criterion, the flame artifact length, which was evaluated only in bone window images, was 26 mm on average (standard deviation  $\pm 9.78$ ) (minimum:8, maximum:54 mm) in standard imaging, whereas it decreased to 3.66 mm (standard deviation  $\pm 2.54$ ) (minimum:0, maximum:7 mm) in reconstructions via SMAR.

## Discussion

Metallic artifacts in spinal and cranial CTs can be caused by stabilization instruments, foreign bodies, metallic materials used in cranioplasty, aneurysm clips, endovascular embolization coils, dental prostheses, and fillings (5). The prevalence of spinal stabilization surgeries has increased over the years, and accordingly, artifacts caused by the used instruments are encountered more commonly (1,2). The first study on MAR was conducted by Kalender et al. (6). Although there have been significant improvements in CT image quality over the last decade, the metal artifact problem has not been eliminated. Artifacts caused by metal implants generate different degrees of severity depending on the shape, size, and variety of the metals used.

Depending on its location, it impairs the image quality of adjacent critical anatomical structures. It restrains the ability to make clear decisions for evaluating physicians and reduces the diagnostic value of CT (7). It limits the evaluation of conditions such as adjacent SC, NF, P-PA anatomy and pathologies, fracture and loosening of the instrumentation material in lumbar metallic materials (3). Thus, CT manufacturers have developed special patented MAR systems to reduce the losses caused by artifact in images and increase the diagnostic value of the captured CTs. The most used commercial patented MAR methods in CT imaging in the presence of clinical real metal implants are as follows: SEMAR (single-energy MAR, Canon Medical Systems, Otawara, Japan), O-MAR (orthopedic MAR, Philips Healthcare, Best, Netherlands), SMAR and MARS (Smart MAR and MAR Sequence, respectively, GE Healthcare, Milwaukee, WI/USA), and MARIS and iMAR (MAR in Image Space and iterative MAR, respectively, Siemens Healthineers, Erlangen, Germany) (7,8).

It is the SMAR (Smart MAR, GE Healthcare, Milwaukee, WI/USA) software, which was used in our study. Smart MAR algorithm firstly identifies the metal in an image, the metal is then removed, and a “metal mask” is generated. An image without metal is then reconstructed, and finally, the metal identified in the first stage is placed over the new images as a “metal mask” (9).

Metal artifact formation occurs thanks to the contribution of beam hardening, scatter, noise, photon starvation, and edge effects. Beam hardening results in dark streaks between high attenuating objects. The scattering shifts the direction of the photons. Noise and photon starvation can be seen in metals with high density and metals with high atomic numbers. This results in completely white dark lines in the final reconstructed image involving the metal (7,10).

In the literature, the number of publications on the effects of various MAR technologies on implant-related CT artifacts on patients is limited. Most studies evaluating MAR algorithms have evaluated orthopedic hardware (such as prostheses) in phantoms, and generally, these studies do not have spinal fixations (3). Besides, most of the studies published on MAR in the literature are the studies conducted with dual-energy CT (5,11).

It has been revealed in the pilot study of Kotsenas et al. (3) that the IMAR reconstruction technique is crucial in visualizing critical anatomical structures such as SC and adjacent paravertebral soft tissues. In addition to that, this technique has been reported to reduce the linear “flame”

artifact size and enhance the visualization of the vertebral body cortex. Radiologists in this study suggested routine reconstruction of IMAR images in 90% of cases (3). Wang et al. (5) utilized MAR algorithms, which have been generated using dual-energy virtual monochromatic kilo electron volt (keV) images in 18 patients with metal spinal fusion and stabilization material. They conducted the image quality assessment with a subjective 5-point image quality scale, as in our study (5). In this study, screw widths were tried to be measured, and measurements could be achieved with small errors over 100 keV.

The radiation dose distribution administered to the patients in our study ranged between 3.23 and 14.1 mSv (mean=8.95 mSv). In the study of Kotsenas et al. (3), like our study, the radiation dose distribution was reported to be between 5.9 and 40.7 milli Grays (mean=19.6 mGy) (1 mGy=1mSv, updated dose unit mSv). In another study by Aissa et al. (12), the radiation dose was reported as 1.7-34.9 mGy (mean=15.9). These doses are considerably high compared to our study. The reason for this may be the significant reduction in radiation doses administered to patients in all CT examinations thanks to the significant developments in CT technology compared to 2012-2013 when the Kotsenas’s study was conducted and 2015-2016 when the Aissa’s study was conducted, and/or the use of different brands of CT scanners.

In our study, the worst score from the obtained images was attained as 1 in the SC evaluation in the standard imaging that was performed in the soft tissue window. This score increased to 3 when the SMAR reconstruction was conducted. The best scores were obtained in NF and P-PA evaluation on images with SMAR reconstruction in the bone window, with 5. Although the increase in bone cortex visualization score was more limited, all the score changes between standard and SMAR reconstruction were determined to be significant ( $p<0.0001$ ). Flame artifacts of different lengths were observed in all patients in standard imaging, whereas no flame artifact was observed in 6 (25%) patients in reconstructions with SMAR. Regarding the flame artifact, a remarkable decrease was determined in the size of the artifact between standard and SMAR images (from 26 mm to -3.66 mm), and the difference ( $p<0.0001$ ) was statistically significant as well. It can be suggested that the SMAR technique is successful, particularly in flame artifacts. Our results were found to be compatible with the literature (3,13). Among the critical anatomical structures, the SC score is lower than the NF and P-PA scores in all evaluated imaging parameters. Hence, it can be stated

that metal artifact makes SC evaluation most difficult. This finding has been confirmed by Kotsenas et al. (3) as well.

In our study, in which the scores of 3 and above were considered as diagnostically significant, it is noticed that it is impossible to perform an adequate and safe radiological diagnostic evaluation in SC and P-PA images, which were 1 and 2 points, respectively, in soft tissue standard imaging. On the other hand, with the application of SMAR reconstruction to the same images, these scores increased to 3 for SC and 4 for P-PA; thus, it has gained an improvement that will allow diagnostic evaluation.

Metallic artifact is related to density, and less CT artifact is generated from less dense materials. The artifact density created by the materials is as follows: plastic<titanium<vitallium<stainless steel<cobalt-chromium (2). It has been revealed that the type of metal used in spinal stabilization and the application site may have an impact on MAR performance. Hence, to achieve the best results, it might be important to have the specific metal types and the MAR algorithms to be applied to these metals instructed by the vendors (13).

MAR algorithms are used to reduce cranial deep brain stimulation artifacts as well as improving spinal and other orthopedic prosthesis/implant artifacts (14). It is also helpful in reducing aneurysm clip-coil artifacts and enhancing image quality in axial CT and CT angiography (15,16). In this way, the number of invasive procedures could be reduced. Nonetheless, DSA angiography remains the gold standard for now (15).

Contrary to these, it has been suggested that none of the MAR technologies are useful for heterogeneous, metal-dense dental filling artifacts, even creating new artifacts (17).

## Conclusion

The MAR technique significantly reduces the artifacts occurring with standard techniques in adjacent tissues in the presence of metal implants applied for medical treatment purposes and allows a clearer evaluation of this region by the radiologist. The use of this technique in the presence of metal in the scanned area enhances the quality of CT images and the diagnostic value of radiological examination. However, there is a need for the development of MAR software for optimal imaging, albeit they provide significant improvement in metallic artifacts compared to standard images.

## Acknowledgments

The authors thank Assistant Prof. Dr. Utku Alkara and Associate Prof. Dr. Burak Eren for their help on this study. This research did not receive any specific grant from funding agencies in the public, commercial, or not-for-profit sectors.

## Ethics

**Ethics Committee Approval:** This study was performed in line with the principles of the Declaration of Helsinki. Approval was granted by the Ethics Committee of İstanbul Yeni Yüzyıl University (date: 05.04.2021/no: 2021/04-653).

**Informed Consent:** Written informed consent was obtained from the patients/ legal guardians for publication of this case report and any accompanying images.

**Peer-review:** Externally peer-reviewed.

## Authorship Contributions

Concept: N.S.B., S.B., Design: N.S.B., S.B., Data Collection or Processing: N.S.B., S.B., Analysis or Interpretation: N.S.B., S.B., Literature Search: N.S.B., S.B., Writing: N.S.B., S.B.

**Conflict of Interest:** No conflict of interest was declared by the authors.

**Financial Disclosure:** The author declared that this study has received no financial support.

## References

1. Martin BI, Mirza SK, Spina N, Spiker WR, Lawrence B, Brodke DS. Trends in lumbar fusion procedure rates and associated hospital costs for degenerative spinal diseases in the United States, 2004 to 2015. *Spine (Phila Pa 1976)* 2019;44(5):369-376.
2. Malhotra A, Kalra VB, Wu X, Grant R, Bronen RA, Abbed KM. Imaging of lumbar spinal surgery complications. *Insights Imaging* 2015;6(6):579-590.
3. Kotsenas AL, Michalak GJ, DeLone DR, Diehn FE, Grant K, Halaweish AE, et al. CT metal artifact reduction in the spine: can an iterative reconstruction technique improve visualization? *AJNR Am J Neuroradiol* 2015;36(11):2184-2190.
4. Stradiotti P, Curti A, Castellazzi G, Zerbi A. Metal-related artifacts in instrumented spine. Techniques for reducing artifacts in CT and MRI: state of the art. *Eur Spine J* 2009;18(Suppl 1):102-108.
5. Wang Y, Qian B, Li B, Qin G, Zhou Z, Qiu Y, et al. Metal artifacts reduction using monochromatic images from spectral CT: evaluation of pedicle screws in patients with scoliosis. *Eur J Radiol* 2013;82(8):e360-e366. doi: 10.1016/j.ejrad.2013.02.024.
6. Kalender WA, Hebel R, Ebersberger J. Reduction of CT artifacts caused by metallic implants. *Radiology* 1987;164(2):576-577.
7. Wellenberg RHH, Hakvoort ET, Slump CH, Boomsma ME, Maas M, Streekstra GJ. Metal artifact reduction techniques in musculoskeletal CT-imaging. *Eur J Radiol* 2018;107:60-69.

8. Khodarahmi I, Isaac A, Fishman EK, Dalili D, Fritz J. Metal about the hip and artifact reduction techniques: from basic concepts to advanced imaging. *Semin Musculoskelet Radiol* 2019;23(3):e68-e81. doi: 10.1055/s-0039-1687898.
9. Smart Metal Artifact Reduction (SmartMAR), For Legacy software systems Quick Reference Guide Version 1.0, gehealthcare.com
10. Katsura M, Sato J, Akahane M, Kunimatsu A, Abe O. Current and novel techniques for metal artifact reduction at ct: practical guide for radiologists. *Radiographics* 2018;38(2):450-461.
11. Lee KYG, Cheng HMJ, Chu CY, Tam CWA, Kan WK. Metal artifact reduction by monoenergetic extrapolation of dual-energy CT in patients with metallic implants. *J Orthop Surg (Hong Kong)* 2019;27(2):2309499019851176. doi: 10.1177/2309499019851176.
12. Aissa J, Thomas C, Sawicki LM, Caspers J, Kröpil P, Antoch G, et al. Iterative metal artefact reduction in CT: can dedicated algorithms improve image quality after spinal instrumentation? *Clin Radiol* 2017;72(5):428.e7-428.e12. doi: 10.1016/j.crad.2016.12.006.
13. Guggenberger R, Winklhofer S, Osterhoff G, Wanner GA, Fortunati M, Andreisek G, et al. Metallic artefact reduction with monoenergetic dual-energy CT: systematic ex vivo evaluation of posterior spinal fusion implants from various vendors and different spine levels. *Eur Radiol* 2012 ;22(11):2357-2364.
14. Nagayama Y, Tanoue S, Oda S, Sakabe D, Emoto T, Kidoh M, et al. Metal artifact reduction in head ct performed for patients with deep brain stimulation devices: effectiveness of a single-energy metal artifact reduction algorithm. *AJNR Am J Neuroradiol* 2020;41(2):231-237.
15. Kuroda H, Toyota S, Kumagai T, Iwata T, Kobayashi M, Mori K, et al. Feasibility of smart metal artifact reduction algorithm on computed tomography angiography for clipping of recurrent aneurysms after coil embolization. *World Neurosurg* 2019;127:e1249-e1254.
16. Zopfs D, Lennartz S, Pennig L, Glauner A, Abdullayev N, Bremm J, et al. Virtual monoenergetic images and post-processing algorithms effectively reduce CT artifacts from intracranial aneurysm treatment. *Sci Rep* 2020;10(1):6629.
17. Huang JY, Kerns JR, Nute JL, Liu X, Balter PA, Stingo FC, et al. An evaluation of three commercially available metal artifact reduction methods for CT imaging. *Phys Med Biol* 2015;60(3):1047-1067.